forum acusticum 2023

ON A SIMPLIFIED PREDICTION MODEL OF THE DYNAMIC MOBILITY OF SOLID BUILDING ELEMENTS WITH EXPERIMENTAL VALIDATIONS

Yohko Aoki[1*] **Korbinian Schwab**[2] **Sven Öhler**[1] **Bernd Kaltbeitzel**[1]
[1] Fraunhofer Institute for Building Physics IBP, Nobelstr. 12, 70569 Stuttgart, Germany
[2] Technical University of Munich, Building Physics, Arcisstraße 21, 80333 München, Germany

ABSTRACT

Standard EN 12354-5 describes the prediction method of the noise due to building equipment. The characteristics of the noise source and the connected building element can be determined according EN 15657, which suggests using a point mobility of an infinite homogeneous plate as the mobility of the building element. However, this characteristic mobility is frequency constant, and differs at low frequencies significantly from the dynamic mobility of the finite plate, particularly near the boundaries. Such an oversimplified model leads to the incorrect estimation of the noise from building equipment. To improve the accuracy without deteriorating its simplicity, a simplified dynamic model is developed, in which the mobility at low frequencies is expressed as a linear function of frequency, while the mobility at mid and high frequencies is still determined by the frequency-constant model. The linear mobility function relies on the material and the geometry of the plate, the location of the source on the plate and the supporting structures affecting the boundary conditions. In particular, this paper focuses on the effects of locations and boundary conditions on the gradient of the linear mobility functions. This simplified prediction model was validated with the measured dynamic point motilities of several building elements.

Keywords: *mobility, structure-borne noise, EN12354-5*

1. INTRODUCTION

Standard EN 12354-5 [1] describes the prediction method of the noise due to building equipment, such as a bathtub and a shower tray. The characteristics of the noise source and the receiving building element can be determined according EN 15657 [2], which suggests using a collocated point mobility of an infinite homogeneous plate as the mobility of the building element [3],

$$Y_{char} = \frac{1}{8\sqrt{\rho h D}}, \quad (1)$$

where ρ denotes the density, h is the thickness, and D is the bending stiffness of the building element, respectively. This characteristic mobility is frequency constant and differs at low frequencies significantly from a frequency dependent complex mobility function of the finite plate, particularly near the boundaries. Such an oversimplified model leads to the incorrect estimation of the noise from building equipment, particularly because building equipment are often placed at the corner of the room.

Therefore, EN 12354-5 [1] includes the simple asymptotic formulas of the real part of the mobility at corner and edge positions, in addition to the characteristic mobility. The analytical derivation of these asymptotic expressions as well as the additional imaginary part of the mobility can be found in Petersson *et al.* [4]. This paper introduces a different approach based on the mobility with the modal summation method.

At frequencies well below the 1st resonance frequency, the magnitude of the mobility follows an almost straight line in double logarithmic scale. To improve the accuracy without deteriorating its simplicity, this paper proposes to use that straight line to predict the point mobility of the receiver at low frequency. The straight line in double logarithmic scale can be given in linear scale as follows

$$Y_{lin} = a_{lin}(r_s, D, \rho, h, \dots)\, f^N, \quad (2)$$

[*] ***Corresponding author***: yohko.aoki@ibp.fraunhofer.de

where a_{lin} is the frequency constant coefficient, which depends on the material, the geometry, and the boundary condition of the building elements, as well as the location of the collocated force velocity pair on the plate. This coefficient is positive real, and subsequently the linear mobility becomes a real positive function, as the characteristic mobility. The frequency is denoted by f, and its exponent, N, is related to the boundary condition of the plate and is defined in the distinct range between $-1 \leq N \leq 1$, dependent on the boundary condition. When the transverse displacement of the plate along its boundary is ideally constrained, i.e., simply supported or clamped, N is set to be 1, i.e., the mobility function linearly increases with frequency. On the other hand, when a panel is freely suspended, N is set to be - 1, i.e., the mobility function is inverse proportion to frequency. When the transverse motion along the boundary is resiliently supported, the exponent varies between -1 and 1, the mobility function is dependent on the stiffness of the resilient support. In reality, the transverse motion of building elements can never be perfectly constrained but is often negligible. Therefore, this paper focuses on the case with N=1, where the transverse movement along the boundary is practically constrained. In this case, the coefficient a_{lin} refers to the gradient of the linear mobility function in Eq. (2).

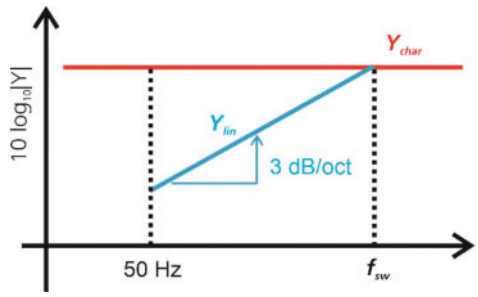

Figure 1. Concept of the hybrid point mobility, the linear mobility (Y_{lin}, light blue) in combination with the characteristic mobility (Y_{char}, red) and the switching frequency f_{sw}.

Figure 1 shows the concept of the hybrid mobility model in double logarithmic scale: the mobility at low frequencies is predicted by Eq. (2), while the mobility at mid and high frequencies is still determined by the frequency-constant model in Eq. (1). The linear mobility model switches to the characteristic mobility at the crossing frequency (switching frequency f_{sw}) of these two functions,

$$f_{sw} = \frac{Y_{char}}{a_{lin}}. \qquad (3)$$

Thus, the amplitude of the hybrid mobility never exceeds the characteristic mobility. The switching frequency f_{sw} is expressed as the inverse proportion of the gradient, and thus the overestimation of the gradient results in the underestimation of the switching frequency. For example, doubling the gradient leads to the shift of f_{sw} in one octave towards lower frequencies.

As shown in Fig 1, it is common to express the mobility in decibel scale, either $10\log_{10}|Y|$ or $20\log_{10}|Y|$ [5]. This paper uses $10\log_{10}|Y|$ in accordance with the prediction method in EN 12354. Thus,

$$10\log_{10}\left|\frac{Y_{lin}}{Y_0}\right| = 10\log_{10}|a_{lin}| + 10\log_{10}|f|, \qquad (4)$$

where the nominal mobility is Y_0=1 m/(Ns). Using dB scale in Eq. (4), the gradient of the linear mobility function appears as the intersection to y-axis, while the gradient is constant in double logarithmic scale, +3 dB per octave.

This paper focuses on derivation of the gradient of the linear mobility from the dynamic mobility. In chapter 2, the analytical model of the dynamic mobility is validated with reference to the measured point mobility. In Chapter 3 the gradient of the linear mobility is derived by the dynamic mobility model. The formula of the gradient is simplified step by step to achieve a practical calculation model with little computational cost. The effects of the location and the boundary condition on the gradient of the linear mobility were investigated. In chapter 4, the idea of the hybrid model was validated with reference to the measured installation noise of a shower tray.

2. MOBILITY OF THE CONCRETE FLOOR

The driving point mobility between the collocated velocity v_s and the force f_s at (x_s, y_s) of a homogeneous, thin rectangular plate is expressed by the modal summation method [5]

$$Y_{v_s,f_s}(\omega) = \frac{v_s(\omega)}{f_s(\omega)} = j\omega \sum_{r=1}^{\infty} \frac{\phi_r^2(x_s)\,\phi_r^2(y_s)}{M_r[(1+j\eta)\omega_r^2 - \omega^2]}, \qquad (5)$$

where ϕ_r, M_r and ω_r denote the r^{th} mode shape function, the modal mass, and the eigen-frequency, respectively. The analytical formulas of these values in case of the ideal boundary conditions are given in many references, for example in [5]. η is the loss factor of the building element. In practice, it is acceptable to truncate the mode set at R, which is the highest modes resonating in the frequency of interest, because the modal contributions decrease with the difference between their natural frequencies and the excitation frequency.

In reality, the building elements are resiliently supported by the carrying structural elements. Such boundary conditions can be modelled using linear and rotational springs along the boundaries [5]. When ideal massless, linear and rotational

springs connect the plate edges to the infinite baffle, the counter force F_r, and the counter moment M_r are generated along the boundary under the primary excitation:

$$F_r(\omega) = -k_L(1 + i\eta_B)\, w(\omega), \quad (6a)$$

$$M_r(\omega) = -k_R(1 + i\eta_B)\, \theta_{x,y}(\omega), \quad (6b)$$

where k_L and k_R are the linear and rotational stiffness used with the boundary loss factor, η_B. w and $\theta_{x,y}$ denote displacement and angular rotation of the plate along the boundary. The velocity at (x_s, y_s) is expressed by the linear summation of the responses due to the primary force and the counter forces and moments:

$$v_s = Y_{v_a,f_s}\, f_s + Y_{v_s,F_r} F_r + Y_{v_s,M_r} M_r\,, \quad (7)$$

where $Y_{vs,Fr}$ and $Y_{vs,Mr}$ are respectively the mobility functions between the velocity and the force, and between the velocity and the moment along the boundaries. Finally, the modified point mobility between the collocated velocity and the force is derived by solving the above formulas with reference to the primary force. For more details, see [5].

The blue line in Fig. 2 shows the measured mobility function of the floor in the testing facility room P9 of the Fraunhofer Institute for Building Physics IBP in Stuttgart. The floor is made out of concrete and is supported by limestone walls. The excitation force is generated by the inertial shaker placed at (1.78, 0.25) m from the corner. The transverse motion of the floor is measured by the two accelerometers placed very close to the shaker (See Fig. 3). The point mobility is predicted as an average of two mobilities. The geometry and the material parameters of the floor in P9 are summarized in Table 1.

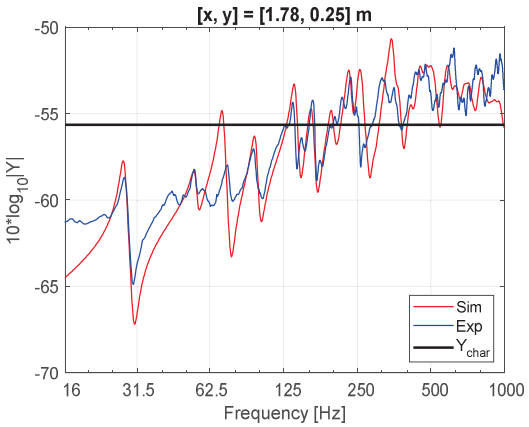

Figure 2. Measured (blue thin) and simulated (red thin) point mobility at (1.78, 0.25) m, and the characteristic mobility (black solid) in P9.

Figure 3. The shaker with the force transducer and two accelerometer sensors.

The red line in Fig. 2 is the simulated mobility of the resiliently supported plate using Eq. (7). The boundary stiffness is the numerically predicated by minimizing the absolute difference between the simulated first three eigen-frequencies and the measured ones, while material parameters of the floor were kept constant. The estimated boundary parameters are shown in Table 1. The linear stiffness is high enough to conclude that the transverse displacement is practically constrained, while the rotational motion is only softly constrained [6]. Such boundary condition can be practically considered as the simply supported plate with gentle rotational constraints.

Table 1. Geometrical and material parameters in P9.

Variables		value	Unit
Structure	Size	4.96 × 3.96	m
	Thickness	0.14	m
	Elastic Modulus	27.5	GPa
	Poisson's Ratio	0.20	---
	Loss Factor	0.05	---
	Density	2300	kg/m^3
	$f_{sw,max}$	0.7264	kHz
Simulated Boundary	Linear stiffness	1×10^9	N/m^2
	Rot. Stiffness	3.79×10^6	N
	Loss Factor	0.1	---

The measured and simulated mobility agree quite well up to 250 Hz, and above that frequency, the overall amplitudes still agree fairy well, though the peaks and dips don't fit perfectly. Obviously, the amplitude of both measured and simulated point mobilities is far lower than the characteristic mobility

up to around 125 Hz. At 50 Hz, the lowest frequency limit of interest in building acoustics, the dynamic mobility is approximately 10 dB lower than the characteristic mobility. This result confirms that the characteristic mobility needs to be improved at low frequency.

3. HYBRID MODEL

3.1 Gradient of the linear mobility

The gradient of the linear mobility model in Eq. (2) is given by the limit of the first derivative of the amplitude of the dynamic mobility as the frequency approaches zero. Assuming that the loss factor η is negligible, and the first eigen frequency of the plane is larger than zero, $\omega_1>0$, the mobility function becomes a positive imaginary number below the first resonance frequency. Thus, the gradient is expressed as follows

$$a_{r,s} = \lim_{\omega \to 0} \frac{d|Y|}{d\omega} \approx \sum_{r=1}^{R} \frac{\phi_r^2(x_s)\,\phi_r^2(y_s)}{M_r \omega_r^2}. \quad (8)$$

Away from the center of the plate, the mobility decreases, and it becomes theoretically zero along the ideally constrained boundary, although it can never be zero under real circumferences. Therefore, it is important to define the practical lower limit of the mobility to avoid extreme underestimation due to the idealized boundary condition, although the simulated mobility can fall below that limit. Moorhouse *et al.* in [7], have derived a formula of the upper envelope curve of the dynamic mobility to include the resonant peaks. That upper envelop leads the lower limit of the mobility as shown below [1]

$$Y_{min}(\omega) = \frac{Y_{char}}{\coth\left(\frac{1}{\beta(\omega)}\right)}, \text{ where } \beta(\omega) = \frac{4}{\omega \eta M Y_{char}}, \quad (9)$$

and M is the mass of the receiving structure. Unlike the characteristic mobility, the lower limit is expressed as a function of frequency. The linear mobility must be higher than Y_{lim} at the lowest frequency range of interest. Thus, the lower limit of the gradient is derived as

$$a_{min} = \frac{Y_{min}(f_{Lim})}{f_{Lim}}. \quad (10)$$

In this paper, f_{Lim} is set to be 50 Hz, the lowest frequency range of interest in building acoustics. Theoretically any other frequency can be applied.

The gradient of the linear mobility function does not offer the intuitive information to evaluate the amplitude of the mobility. Therefore, the switching frequency of the hybrid mobility model is presented instead of the gradient. By inserting Eq. (10) into Eq. (3), the upper bound of f_{sw} can be predicted using the minimum gradient,

$$f_{sw,max} = \frac{Y_{char}}{a_{min}}. \quad (11)$$

This is 724 Hz for the considered plate in this chapter (P9 in Table 1). Above this upper frequency limit, the characteristic mobility is always used as the receiver mobility. The lower limit of f_{sw} is set to be f_{Lim} = 50 Hz.

3.2 Effect of the location conditions

Figure 4 shows the effect of the source location on the switching frequency of the linear mobility. The x-axis is the distance between the plate corner and the predicted point (r_d), normalized by the length of the diagonal line of the plate (L_{diag}). The lower and upper bounds of f_{sw} are plotted in black solid lines. Both the blue (simply supported plate) and the red lines (clamped plate) monotonically decrease as the point approaches the center of the plate. Near the center, f_{sw} falls below 50 Hz. Thus, the characteristic mobility is sufficient in the middle of the plate. On the other hand, f_{sw} is higher than 50 Hz near the edge, and hence the hybrid model is required at low frequency. Very close to the edge, at around r_d/L_{diag} = 0.05 and 0.08 for pinned and clamped plates, f_{sw} exceeds the upper bound given by Eq. (11).

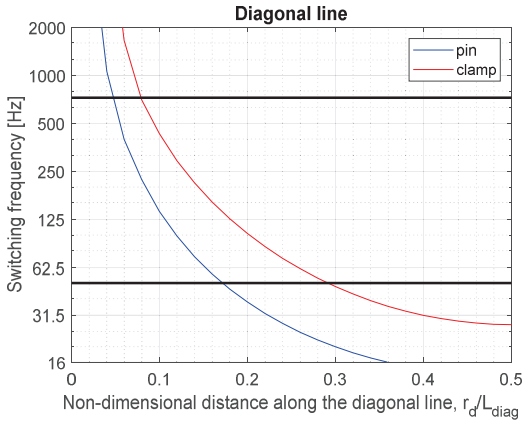

Figure 4. The switching frequency along the diagonal line from the corner to the center of P9 floor: simply supported (blue) and clamped boundary conditions (red). The upper and lower bounds of f_{sw} (black solid lines).

In Figure 5, the rectangular plate is colored in blue and white: the area highlited in blue requires the hybrid model, while that in white not above 50 Hz. For the outer area of the blue contour, the hybrid mobility is required in case of the simply supported condition. The red contour is the border for the clamped boundary condition. This image implies that the area near the edge always needs model

refinement, while the characteristic mobility is sufficient at the middle of the plate.

Along the blue or red border line in Fig. 5, the switching frequency is constant at 50 Hz. The border roughly follows the concentric rectangular of the plate (dotted rectangles), though the corners are rounded. This result leads to the idea to use the identical switching frequency along the concentric rectangular. The nominal value is predicted at the midpoint of the edge of the concentric rectangular along the perimeter. It must be noted that, this "midpoint" model is prone to underestimate the switching frequency, as f_{sw} is lowest at the midpoint, and increases as the point gets closer to the edge, as shown in Fig. 4.

Assuming $x_s<L_x/2$ and $y_s<L_y/2$, and the ratio of x- to y-coordinates of the measuring point, x_s/y_s, is bigger than the aspect ratio of the rectangular plate, the gradient of the linear mobility function at (x_s, y_s) is simplified as to

$$a_{r,m} = \lim_{\omega \to 0} \frac{d|Y|}{d\omega} \approx \sum_{r=1}^{R} \frac{\phi_r^2(x_m)\,\phi_r^2(y_s)}{M_r \omega_r^2}\,, \qquad (12)$$

where x_m denotes the x-coordinate of the center of the plate, $x_m=L_x/2$. When the ratio x_s/y_s, is smaller than the plate aspect ratio, the gradient should be calculated at (x_s, y_m), where $y_m=L_y/2$. The aspect ratio of the plate is expressed by

$$AR = L_x/L_y\,, \qquad (13)$$

where L_x and L_y are the side length of the panel along x, and y-axis, respectively.

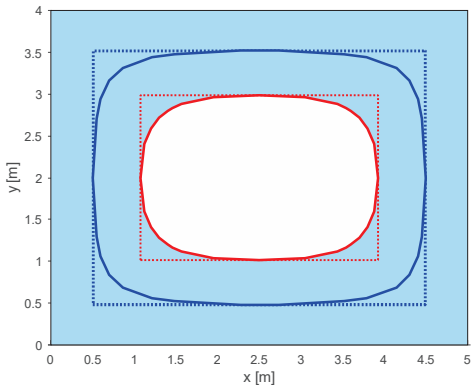

Figure 5. The sketch of the plate with the border of the areas, where the linear model is required, and not required above 50 Hz (solid line): blue (simply supported), red (clamped).

3.3 Boundary conditions

Figure 4 also indicates that f_{sw} of the clamped plate is higher than that of the simply supported plate. The difference between two ideal boundary conditions increases as the source location gets closer to the edge. It means that the boundary condition plays more important role near the edges.

Figure 6 shows the effect of the rotational stiffness along the border of the simply supported plate on the switching frequency of the mobility. The rotational stiffness is normalized by the following parameter [6]

$$k_0 = D/L_x\,. \qquad (14)$$

The switching frequency monotonically increases with the rotational stiffness, and it follows a sigmoid curve shape. While the rotational stiffness is low, f_{sw} agrees with that of the simply supported plate. As the stiffness increases, the switching frequency gets closer to that of the clamped plate. The difference between the lowest and the highest value expands as big as nearly four octaves. The red marker refers to f_{sw} of the measured mobility function in Fig. 2 at the estimated rotational stiffness given in Table 1. The gradient of the measured mobility function is estimated using the linear regression analysis. The red marker is not aligned exactly on the blue curve, but slightly lower, because the transverse displacement along the edges is not ideally constrained in reality.

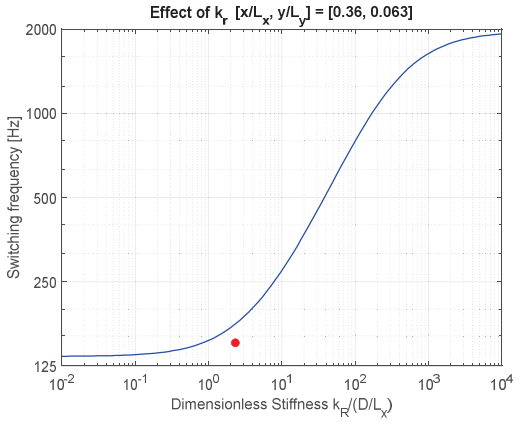

Figure 6. Blue line: f_{sw} with reference to the rotational stiffness of the plate at (1.78, 0.25) m. Red dot: the measured f_{sw} with reference to the estimated rotational stiffness.

3.4 First order estimation of the gradient

Up to this point, the gradient was estimated by using the complete set of modes. It means that, the effort to calculate the gradient is as high as the effort to predict the dynamic point mobility itself. Therefore, the linear mobility model does not bring any advantage in terms of the simulation costs.

To further simplify the model in addition to the contour method in the previous section, the infinite number of vibration modes are truncated, and only the first mode is taken into account. In combination with both simplification methods, the gradient is expressed by

$$a_{1,m} = \lim_{\omega \to 0} \frac{d|Y_1|}{d\omega} \approx \frac{\phi_1^2(x_m)\,\phi_1^2(y_s)}{M_1 \omega_1^2}. \quad (15)$$

Figure 7 compares the switching frequencies of the simply supported plate using the rigorous calculated gradient (blue solid) by Eq. (8) with that derived by the simplified first mode method (blue dotted) given in Eq. (15). The mobility is predicted along x-axis at y = 0.25 m (y/L_y = 0.063), and thus the dotted line terminates at x/L_x = 0.063, which is the corner of the concentric rectangular. Near the center of the plate, f_{sw} of the first mode method is higher than that predicted by using the rigorous model, because this simplified method always underestimates the mobility, and the underestimated mobility leads to the higher switching frequency. On the other hand, as shown in the previous section, the switching frequency of the rigorous model increases as the point gets closer to the edges. Finally, near the edge, these two effects, "overestimation" due to mode truncation and "underestimation" due to midpoint estimation, compensate each other, and at one point the rigorous value can be equal to the simplified value. In Fig. 7, these two curves cross at the termination point of the dotted line. Therefore, in general, this model gives good estimation near the corner, but not always along the edges.

In Fig. 7, the switching frequency of the five measured mobility functions are also plotted by red solid points. These red points are fairly well aligned on the red curve (the simulated switching frequency of the resiliently supported plate). As discussed in Section 2, the estimated boundary condition can be practically considered as the ideal simply supported boundary with gentle rotational constraints. Nevertheless, the red line (resilient support) appears below the blue curve (simply supported). Furthermore, the blue solid line exceeds the upper bound (black solid) and keeps increasing very sharply as getting closer to the corner, while the red line remains under the upper bound. It implies that the imperfect constraint of the transverse displacement is not negligible near to the border, and the upper bound given by Eq. (11) offers a good practical limit.

As shown in Figure 6, f_{sw} increases with the stiffness of the rotational spring. Therefore, the effect of the imperfect linear constraint is partly compensated by the additional stiffening effect due to rotational springs. In combination with both effects, the simply supported boundary condition offers a decent estimation of a real boundary condition, which is modelled as very stiff linear springs and soft rotational springs.

Therefore, in this paper the simply supported boundary is applied to estimate the mobility of the real building. Finally, the gradient of the linear mobility is given as

$$a_{1,m,Pin} = \frac{4}{M\omega_1^2}, \text{ where } \omega_1^2 = \frac{D}{\rho}\pi^4\left(\frac{1}{L_x^2} + \frac{1}{L_y^2}\right)^2. \quad (16)$$

It must be noted that this simplification may lead to either over or underestimation, dependent on the real boundary condition. As the real boundary condition becomes more constraint, this method tends to underestimate the switching frequency, and vice versa.

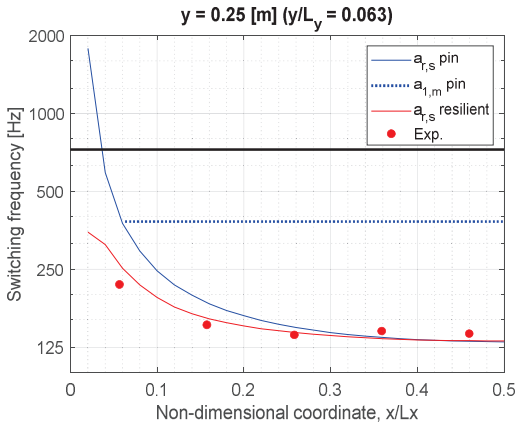

Figure 7. f_{sw} along y = 0.25 m (y/L_y = 0.063): first order model (blue dotted), and rigorous model simply supported (blue thin) or resiliently supported (red thin). The measured f_{sw} along y = 0.25 m in P9 (red dots). The upper bound of f_{sw} (black solid lines).

4. EXPERIMENTAL VALIDATION WITH A SHOWER TRAY

4.1 Experimental Setup

For a validation of the concept, the suggested hybrid mobility model is applied to predict the structure-borne sound via the building element. As shown in Fig. 8, a 0.9 m quadratic shower tray with 8 feet along its edges was placed at the corner of the testing facility room P12 of the Fraunhofer IBP in Stuttgart. The floor is made out of concrete with the thickness of 0.19 m, and its boundary condition was not predetermined. The geometry and the material properties are summarized in Table 2.

The measurements are performed in accordance with DIN EN ISO 10052 and DIN 4109-4, which describes acoustical

measurements of water installations in buildings. The normalized sound pressure level is measured in the receiving room located under the floor, where the shower tray is installed (See Fig. 8). The noise excitation occurs by using a standard source for structure-borne noise (KGN), which is developed and approved by the Fraunhofer Institute for Building Physics. An installation noise standard according to DIN EN ISO 3822-1 [8] is used as a jet nozzle. The KGN is generating a steady jet of water, which hits the shower tray under precisely defined geometrical location, and thus generates a realistic and reproducible installation noise excitation. The use of the KGN, as a consistent source of excitation, enables a comparison of the noise behavior of different sanitary objects. The KGN is operated with a pressure of 0.3 MPa and a steady water flow of 0.25 L/s (±4 %). Compared to the generated sound level, the excitation by a KGN is the upper limit of commercial shower heads and draw-off taps.

Table 2. Geometrical and material parameters in P12.

Variable	Value	unit
Size	5 × 3.42	m
Thickness	0.19	m
Elastic Modulus	27.5	GPa
Poisson's Ratio	0.20	---
Loss Factor	0.05	---
Density	2300	kg/m^3
$f_{sw,max}$	1.1517	kHz

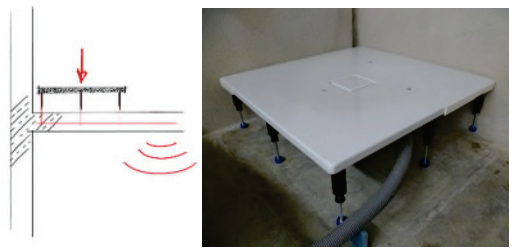

Figure 8. Experimental setup in P12.

4.2 Estimation method and comparison

According to Eq. (18a) in EN 12354-5, the normalized sound pressure level $L_{n,s}$ in the receiving room due to a structure-borne sound source mounted on the supporting building element in the source room is given in dB reference to 2×10^{-5} Pa by

$$L_{n,s} = L_{Ws,inst} - D_{TF} \,, \qquad (17)$$

where $L_{Ws,inst}$ is the installed structure-borne sound power level in dB with reference to 10^{-12} W. D_{TF} is the summation of the residual terms describing the transfer function of the building situation between the input sound power and the output sound pressure level in a receiving room, such as the flanking sound reduction index, and others related to the geometry of the supporting building element. D_{TF} can be analytically predicted for special cases using the formulas given in EN 12354-1 and EN 12354-5 or must be measured in the real building situation. In the considered case, D_{TF} was analytically predicted. Considering the fact that the mobility of the receiving element, 0.19 m concrete floor, is much lower than that of the connected structure-borne sound source, the shower tray can be essentially treated as a force source. Therefore, $L_{Ws,inst}$ is obtained by Eq. (9) in EN 15657,

$$L_{Ws,inst} = 10 \log_{10} \left(\frac{\mathrm{Re}[Y_{R,eq}]}{Y_0} \right) + L_{Fb,eq} \,, \qquad (18)$$

where $L_{Fb,eq}$ is the source single equivalent blocked force squared in dB with reference to 10^{-6} N, measured by the reception plate method. $Y_{R,eq}$ denotes the single equivalent input mobility of the receiver, i.e., the mean value of the point mobility averaged over all 8 contact points of the shower tray to the floor (See Fig. 8). Finally, the normalized sound pressure level in the receiving room is given by

$$L_{n,s} = 10 \log_{10} \left(\frac{\mathrm{Re}[Y_{R,eq}]}{Y_0} \right) + L_{Fb,eq} - D_{TF}. \qquad (19)$$

When the mobility of the receiving element is known, $L_{n,s}$ can be predicted using the above formula.

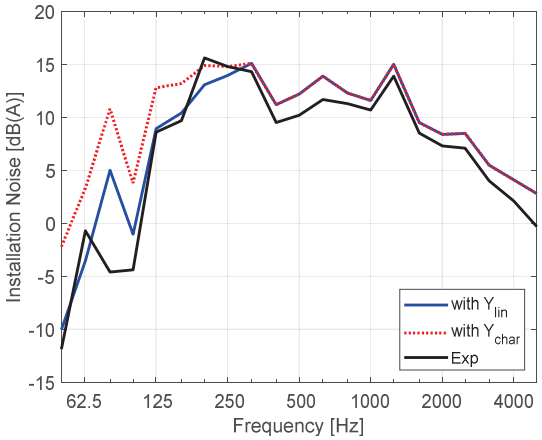

Figure 9. $L_{n,s}$ of a shower tray: Measured (black), and the predicated using the characteristic mobility (red dotted) and using the hybrid model (blue solid).

Figure 9 compares the measured (black) and simulated (red dotted and blue solid) normalized sound pressure levels in one third octave bands. The red dotted line is the estimated

value using the constant characteristic mobility according to Eq. (1), while the blue solid line is derived using the hybrid model. The gradient of the linear mobility function of each foot was calculated using Eq. (16), and then averaged over all feet. Finally, f_{sw} for the hybrid model is predicted according to Eq. (3) as 383.7 Hz. This plot implies that the prediction based on the characteristic mobility overestimates the installation noise at low frequencies up to 15 dB. Using the hybrid first mode model the accuracy of the prediction according EN 12354 was significantly improved, although the boundary condition of the receiving structure was unknown.

5. CONCLUSION

This paper presented the hybrid mobility model to improve the prediction method of the noise due to building equipment. The hybrid mobility model consists of two sections: the mobility at low frequency is predicted by the linear mobility, while the mobility at mid and high frequencies is still determined by the standardized characteristic mobility. The gradient of the linear model is derived as the first derivative of the dynamic mobility function based on the modal summation method. The linear mobility model shifts to the characteristic mobility at the crossing frequency of these two functions, namely the switching frequency, f_{sw}.

The switching frequency of the hybrid model depends on the boundary condition of the building element and the location of the input mobility. Near the edge of the building element, the hybrid model can improve the prediction significantly, although the characteristic mobility model is sufficient around the center of the plate.

To simplify the prediction method, the switching frequency is predicted only at the midpoint of the edge of the concentric rectangular and applied along the perimeter. This simplification is prone to underestimate f_{sw}. To further simply the model, only the first vibration mode of the building element is considered. As the contribution of higher modes is neglected, the truncated mode system always overestimates the switching frequency. Finally, these two effects, "overestimation" due to mode truncation and "underestimation" due to midpoint estimation, and thus the simplest method gives fairly good agreement with the rigorous model near the edge.

Although the boundary condition strongly affects the linear mobility, the boundary conditions of real buildings vary widely, and cannot be precisely estimated. The vertical motion of the building element is very stiffly constrained, but still imperfect, while the rotational motion is only softly constrained, but still not free. Considering that these two effects also compensate each other, the simply supported condition gives quite good estimation of the boundary condition of real building elements.

The hybrid mobility model was validated in a real building situation by predicting the installation noise from a shower tray in a receiving room according EN 12354-5 by using the characteristic mobility and the mobility of the hybrid model for calculation. In comparison with the directly measured value of the sound pressure level, the hybrid model improved the prediction precision significantly instead of using the characteristic mobility.

6. REFERENCES

[1] CEN, European Standard EN 12354-5 (2009): Building acoustics - Estimation of acoustic performance of building from the performance of elements - Part 5: Sounds levels due to the service equipment.

[2] CEN, European Standard EN 15657 (2017): Acoustic properties of building elements and of buildings - Laboratory measurement of structure-borne sound from building service equipment for all installation conditions.

[3] Cremer, L. (2005). *Structure-Borne Sound: Structural Vibrations and Sound Radiation at Audio Frequencies* (3rd *ed.*). Springer Berlin Heidelberg.

[4] Petersson, B. (1993). Structural Acoustic Power Transmission by Point Moment and Force Excitation, Part II: Plate-like Structures. *Journal of Sound and Vibration*, 160(1), 67–91.

[5] Fahy, F. (2006). *Sound and Structural Vibration: Radiation, Transmission and Response* (2nd *ed.*). Elsevier Science & Technology.

[6] Kaito, Y., Honda, S., & Narita, Y. (2018). Identification of elastic edge condition for modeling vibration response of glass touch panel. *Journal of Vibration and Control*, 24(18), 4081–4095.

[7] Moorhouse, A. T., & Gibbs, B. M. (1995). Calculation of the mean and maximum mobility for concrete floors. Applied Acoustics, 45(3), 227–245.

[8] DIN EN ISO 3822-1 (2009): Acoustics - Laboratory tests on noise emission from appliances and equipment used in water supply installations - Part 1: Method of measurement.